Original Research

Effect of mesenchymal stem cells on renal injury in rats with severe acute pancreatitis

Zhiyao Chen, Fengchun Lu, Haizong Fang and Heguang Huang

Affiliated Union Hospital, Fujian Medical University, Fujian, 350001, China
Corresponding author: Heguang Huang. Email: hhuang2@sina.cn

Abstract

The aim of this study was to preliminarily investigate the effect of bone marrow mesenchymal stem cells (MSCs) on structural change of capillary endothelial barrier and expression variation of aquaporin 1 (AQP1) in kidney at the onset of renal injury caused by severe acute pancreatitis (SAP). Ninety male Sprague-Dawley (SD) rats were divided into the control group, the SAP group in which animals received induction of SAP and the MSCs-treated group in which SAP-induced animals were injected with MSCs. They were further subdivided according to the time point that the animals were killed; 6 h, 12 h and 24 h after the closure of the incision, serum, pancreatic and renal samples were collected, respectively. The level of serum amylase (AMY), creatinine (Cr) and blood urea nitrogen (BUN) were analysed, the change of pancreatic histology was assessed, the structural change of the renal interstitial capillaries was evaluated using the transmission electron microscope (TEM) and the location and expression of AQP1 in kidney were analysed using immunohistochemistry, quantitative polymerase chain reaction and Western blot. The outcomes showed that the level of serum AMY, Cr, BUN elevated, the damage of pancreatic tissue and renal capillary endothelial barrier was aggravated and the expression of AQP1 was reduced significantly after induced pancreatitis. But after treatments with MSCs, the elevation of AMY, Cr and BUN was inhibited, the damage of pancreatic tissue and renal interstitial capillary barrier was alleviated and the down-regulation of AQP1 was reversed. In summary, the MSCs therapy could alleviate renal injury in rats with SAP, the mechanism of which might be related to reduction of the damage to renal interstitial capillary endothelial barrier, and up-expression of AQP1 in kidney.

Keywords: Mesenchymal stem cells, severe acute pancreatitis, renal injury, capillary endothelial cell, aquaporin 1

Experimental Biology and Medicine **2013; 238: 687–695. DOI: 10.1177/1535370213490629**

Introduction

Severe acute pancreatitis (SAP) is often complicated by multiple organ failure. The kidney was the second most frequently damaged organ by SAP. Once the acute renal failure (ARF) is present, the mortality is as high as 80%.[1] Studies showed that the excessive activation of inflammatory cytokines and the damage of capillary endothelial barrier could lead to the onset of SAP.[2–4] The structure of endothelial barrier included a monolayer of endothelial cells and basal lamina. The insufficient function of water transportation mediated by endothelial cells could increase capillary permeability in SAP.

Aquaporins (AQP) are a family of water transporting proteins and could selectively mediate water transportation.[5] And the main expression of AQP in the kidney is AQP1. Studies have found that the expression abnormality of AQP1 could lead to a variety of water absorption and filtration dysfunction.[6,7] A recent study has showed that AQP1 in capillary endothelial cells of the pancreas, lung and intestine in rats with experimental acute necrotizing pancreatitis was down-regulated.[8]

Mesenchymal stem cells (MSCs) have received significant attention at present. MSCs could be expanded extensively *in vitro* without loss of function or phenotype.[9] Studies have also shown that MSCs had protective effect on mice with SAP.[10] But whether MSCs have protective effect in renal injury is not investigated yet.

In this study, we sought to explore whether (1) there is structural change of capillary endothelial barrier and expression variation of AQP1 in kidney at the onset of renal injury caused by SAP; and (2) MSCs have protective effect on renal injury induced by SAP through their impact on the capillary endothelial barrier and expression of AQP1 in kidney.

Materials and methods

Animals

Ninety male Sprague-Dawley (SD) rats, weighing 200–250 g, were obtained from the Experimental Animal Center (Shanghai Slac Company, Shanghai, China) and housed in rooms with temperature maintained at $20 \pm 2^{\circ}C$ in 12-h light-dark cycle for at least one week. Food and tap water were provided *ad libitum*.

Culture and identification of MSCs

The cells were cultured by whole the marrow differential adherence method. Confluent cells were dissociated using EDTA-Trypsin (Invitrogen, San Diego, CA) and purified by multiple dissociation and passage. The MSCs from the third generation were acquired for further experiments. Expression of surface markers CD29, CD45, CD90 (Biolegend, San Diego, CA) and CD34 (Santa Cruz Biotechnology, Santa Cruz, CA) of MSCs was confirmed by flow cytometry analysis (FACS; Canto, Becton Dickinson, San Jose, CA).

Preparation of SAP animal model

The induction of SAP was achieved by the method described by Schmidt *et al*.[11] Briefly, the rats were anesthetized by an intraperitoneal injection of 10% Chloral hydrate (3 mL/kg body weight; Bio Basic, Markham, ON, Canada). After a ventral laparotomy, the hepatic duct identified at the hilum of the liver was clamped by a small bulldog clamp, and the biliopancreatic duct was cannulated by a thin polyethylene catheter. Then 5% sodium taurocholate (1 mL/kg body weight; Inalco S.p.A., Milano, Italy) was injected into the biliopancreatic duct at a rate of 0.04 mL/min with a microinfusion pump, and the atraumatic vascular clamp was removed 10 min later. Finally, the abdominal incisions were closed with sutures. The whole procedure was in accordance with the Guide for the Care and Use of Laboratory Animals.[12]

Grouping

Animals ($n = 90$) were divided into three groups according to the animal model and treatment. They were further subdivided according to the time point that the animals were killed: (1) control group at 6 h ($n = 10$): animals were injected with 1 mL normal saline via tail vein at 0 h, and killed at 6 h; (2) control group at 12 h ($n = 10$): animals were injected with 1 mL normal saline at 0 h and 6 h, and killed at 12 h; (3) control group at 24 h ($n = 10$): animals were injected with 1 mL normal saline at 0 h, 6 h and 12 h, and killed at 24 h; (4) SAP group at 6 h ($n = 10$): SAP-induced animals were injected with 1 mL normal saline at 0 h, and killed at 6 h; (5) SAP group at 12 h ($n = 10$): SAP-induced animals were injected with 1 mL normal saline at 0 h and 6 h, and killed at 12 h; (6) SAP group at 24 h ($n = 10$): SAP-induced animals were injected with 1 mL normal saline at 0 h, 6 h and 12 h, and killed at 24 h; (7) MSCs-treated group at 6 h ($n = 10$): SAP-induced animals were injected with 1 mL MSCs (about 1×10^6/mL) via tail vein at 0 h, and killed at 6 h; (8) MSCs-treated group at 12 h ($n = 10$): SAP-induced animals were injected with 1 mL MSCs at 0 h and 6 h, and killed at 12 h; (9) MSCs-treated group at 24 h ($n = 10$): SAP-induced animals were injected with 1 mL MSCs at 0 h, 6 h and 12 h, and killed at 24 h. The 0 h means the moment when abdominal incision was closed.

Detection of serum indicators

Blood samples were collected from the cardiac apex, conserved for 10 min at room temperature, and centrifuged at 3000 g for 10 min at 4°C. The serum was collected and kept at −70°C until measurement. Serum amylase (AMY), creatinine (Cr) and blood urea nitrogen (BUN) levels were determined by using Olympus AV2700 automated clinical biochemistry analysis equipment (Olympus, Tokyo, Japan).

Morphological examination

The body of pancreas was harvested for morphological study. The 10% buffered formalin-fixed sample was embedded in paraffin, sectioned at 4 μm thickness and stained with hematoxylin and eosin (H&E). For electron microscopy, the renal tissues were immediately removed and fixed in the fixation fluid (3% glutaraldehyde–1.5% paraformaldehyde–0.1 M CBS, pH 7.4). Then all samples were sequentially fixed in 1% aqueous osmium tetroxide (OsO4), dehydrated in ethanol, transferred to propylene oxide and embedded in Epon 618. Finally, ultrathin sections (80 nm) were obtained by an ultramicrotome, put on copper grids, stained with uranyl acetate and lead citrate and examined on a transmission electron microscope (TEM; Hitachi, Tokyo, Japan).

Immunohistochemical staining of AQP1 in kidney

Renal tissue was fixed in 10% buffered formalin and processed for embedding in paraffin. Then the sections were dewaxed and rehydrated. High-temperature antigen retrieval was achieved by putting the slides in boiled Citrate buffer (10 mmol/L, pH 6.0) for 20 min and then immersing it in 3% methanol–H_2O_2 for 10 min at room temperature to quench the endogenous peroxidase. Sections were sequentially blocked with 5% BSA at room temperature for 20 min, incubated with anti-AQP1 primary antibody (Abcam, Cambridge, UK) at a dilution of 1:200 for 1 h at room temperature and with secondary antibody (Boster, Wuhan, Hubei, China) for 20 min at room temperature, respectively, and processed by the Streptavidin Biotin peroxidase Complex (Boster, Wuhan, Hubei, China) for 20 min. Sites of peroxidase activity were visualized with DAB. Finally, sections were counterstained with H&E, dehydrated and sealed by xylene transparent neutral resin.

Western blot assay

Dissected nephridial tissues from three different littermates for each group were washed with PBS and total protein was extracted (10 mM Tris base- HCl, 150 mM NaCl, 1% NP-40, 1% Triton X-100, 5 mM EDTA, 0.1% SDS, 1% sodium deoxicholate, 1 mM phenylmethylsulfonyl fluoride, 1 μg/mL aprotinin, 1 μg/mL pepstatin, 1 μg/mL leupeptin,

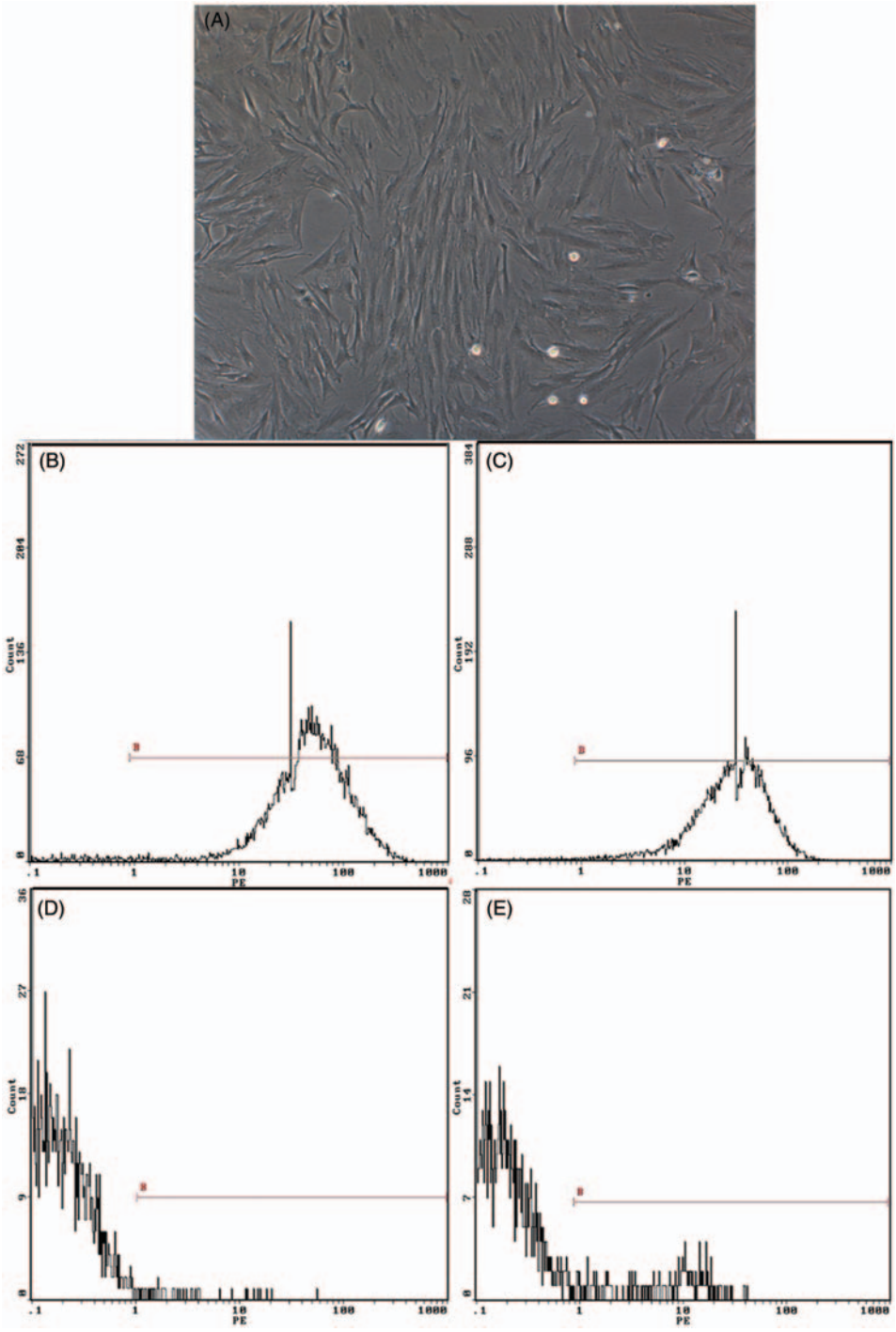

Figure 1 General morphology and expression of surface marker of MSCs. The cell assumed as a spindle-shaped and fibroblast-like appearance, and expanded in the colony form (A). The surface markers of CD29, CD90, CD34 and CD45 were 91.1% (B), 93.5% (C), 0.82% (D) and 2.22% (E), respectively

1% sodium orthonovadate and 50 mM sodium fluoride). The concentration of lysates was determined by the bicinchoninic acid (BCA) assay. Lysates (80 μg) were separated in SDS-polyacrylamide gels and transferred to polyvinylidene fluoride (PVDF). Membranes were blocked with 5% non-fat dry milk and incubated with primary antibody anti-AQP1 (1:2000 dilution), followed by horseradish peroxidase-conjugated secondary antibodies. Immunoblots were developed with ECL (Millipore, Billerica, USA), according to manufacturer's instructions, and densitometric results were analysed with Quantity One image-analysis software (Bio-Rad, Hercules, CA). Coefficients of variance were calculated by the ratio between means ± SE.

RNA extraction and reverse transcription-polymerase chain reaction

Total RNAs were extracted from tissues with TRIzol (Takara, Dalian, China) according to the user's manual.

Table 1 Results of serum amylase, creatinine and urea nitrogen

	6 h	12 h	24 h
Serum amylase control	1025.25 ± 326.93	999.875 ± 212.27	962.25 ± 128.86
SAP	6633.88 ± 846.73*	9421.38 ± 1031.75*	8755.63 ± 734.46*
MSCs-treated	6032.75 ± 534.92†	7475.75 ± 834.18†	6903.38 ± 377.05†
Creatinine control	27.88 ± 3.22	28.75 ± 3.80	27.75 ± 2.33
SAP	55.87 ± 7.13*	92.12 ± 6.33*	148.88 ± 19.50*
MSCs-treated	46.25 ± 8.58†	62.13 ± 7.51†	91.38 ± 10.71†
Urea nitrogen control	7.86 ± 0.84	8.08 ± 1.23	7.64 ± 1.28
SAP	20.26 ± 5.01*	37.25 ± 8.21*	58.36 ± 14.66*
MSCs-treated	14.88 ± 2.12†	26.58 ± 6.22†	32.23 ± 14.22†

After induction of SAP and treatment with MSCs, serum was collected at different time points and assayed for AMY, Cr and BUN levels. The results are shown as the means ± SE ($n = 10$ rats per group).
*$P < 0.01$ vs. the control groups at the same time point.
†$P < 0.05$ vs. the SAP groups at the same time points, as tested using a two-sample *t*-test.

Reverse transcription was done according to the instructions in the ExScript TM RT Reagent Kit, and the reaction conditions were 37°C for 5 min and 85°C for 5 s (Takara, Dalian, China). The PCR reaction for AQP1 was performed with SYBR® Green II RT PCR assay (Takara, Dalian, China) in a total volume of 20 μL reaction system containing: 10 μL of SYBR® Premix Ex Taq™ (1×), 0.4 μL of sense and antisense primers, 0.4 μL of ROX Reference Dye II (50×), 2.0 μL of cDNA and 6.8 μL of dH_2O. Real-time PCR was performed on the ABI 7500 Fast system with the following conditions: 40 cycles with pre-denaturation step at 95°C for 30 s, denaturation step at 95°C for 5 s, extension at 60°C for 30 s. Reference gene is β-actin. Forward primer and reverse primer of target gene AQP1 are 5′-GACTA CACTGGCTGTGGGATCAA-3′ and 5′-CCAGGGCAC TCCCAATGAA-3′, respectively; forward primer and reverse primer of β-sctin are 5′-CCCATCTATGAGG GTTACGC-3′ and 5′-TTTAATGTCACGCACGATTTC-3′.

Statistical analysis

Quantitative data were reported as means ± standard deviation ($\bar{x} \pm S$). Two sample *t*-test was performed to compare the difference of values between two groups, and one-way ANOVA with a post-hoc Fisher's least-significant-difference (LSD) test was applied to identify the significant change of value among several groups. A value of $P < 0.05$ was considered as having statistically significant difference. Statistical analysis was done by using SPSS version 15.0 for windows.

Results

General morphology and expression of surface marker of MSCs

The MSCs attached to the wall of culture vessel after 24–72 h on the average and were cultured in the colony form; the MSCs were purified gradually after several transfers of culture. Under the inverted microscope, the P3 cells assumed a spindle-shaped, fibroblast-like appearance with adherent confluent monolayer morphological characteristics (Figure 1A). The cell surface marker was detected by flow cytometry. The cells expressed high levels of CD 29/90 and low levels of CD 34/45 (Figure 1B–E).

Detection of serum indicators

The results showed that the peak concentration of AMY in the SAP groups was reached at 12 h. The AMY level in the SAP groups was higher than that in the control groups at the corresponding time point, respectively (6 h: $t = 17.52$, $P < 0.01$; 12 h: $t = 21.15$, $P < 0.01$; 24 h: $t = 25.44$, $P < 0.01$). After treatment with MSCs, the AMY level was lower than that in the SAP groups at the corresponding time points (6 h: $t = 5.94$, $P < 0.05$; 12 h: $t = 3.88$, $P < 0.05$; 24 h: $t = 2.40$, $P < 0.05$). The level of Cr was positively time-dependent in the SAP groups and was higher than that in the control groups at the corresponding time points (6 h: $t = 9.47$, $P < 0.01$; 12 h: $t = 22.70$, $P < 0.01$; 24 h: $t = 16.32$, $P < 0.01$). After treatment with MSCs, the level of Cr was lower than that in the SAP groups at the corresponding time points (6 h: $t = 2.28$, $P < 0.05$; 12 h: $t = 8.08$, $P < 0.05$; 24 h: $t = 6.84$, $P < 0.05$). The level of BUN was positively time-dependent in SAP groups and was higher than that in control groups at the corresponding time points (6 h: $t = 6.46$, $P < 0.01$; 12 h: $t = 9.29$, $P < 0.01$; 24 h: $t = 9.12$, $P < 0.01$). After treatment with MSCs, the level of BUN was lower than that in the SAP groups at the corresponding time points (6 h: $t = 2.62$, $P < 0.05$; 12 h: $t = 2.74$, $P < 0.05$; 24 h: $t = 3.39$, $P < 0.05$) (Table 1).

Histopathology of pancreas

The pancreatic damage was aggravated over time after induction of SAP. The damage at 24 h was the most severe at all time points. The pancreatic damage in the SAP groups was more severe than that in the control groups at the corresponding time points, respectively (6 h: $t = 25.2$, $P < 0.01$; 12 h: $t = 35.15$, $P < 0.01$; 24 h: $t = 30.88$, $P < 0.01$). After treatment with MSCs, the damage was less severe than that in the SAP groups (6 h: $t = 4.16$, $P < 0.01$; 12 h: $t = 8.75$, $P < 0.01$; 24 h: $t = 6.01$, $P < 0.01$) (Figure 2).

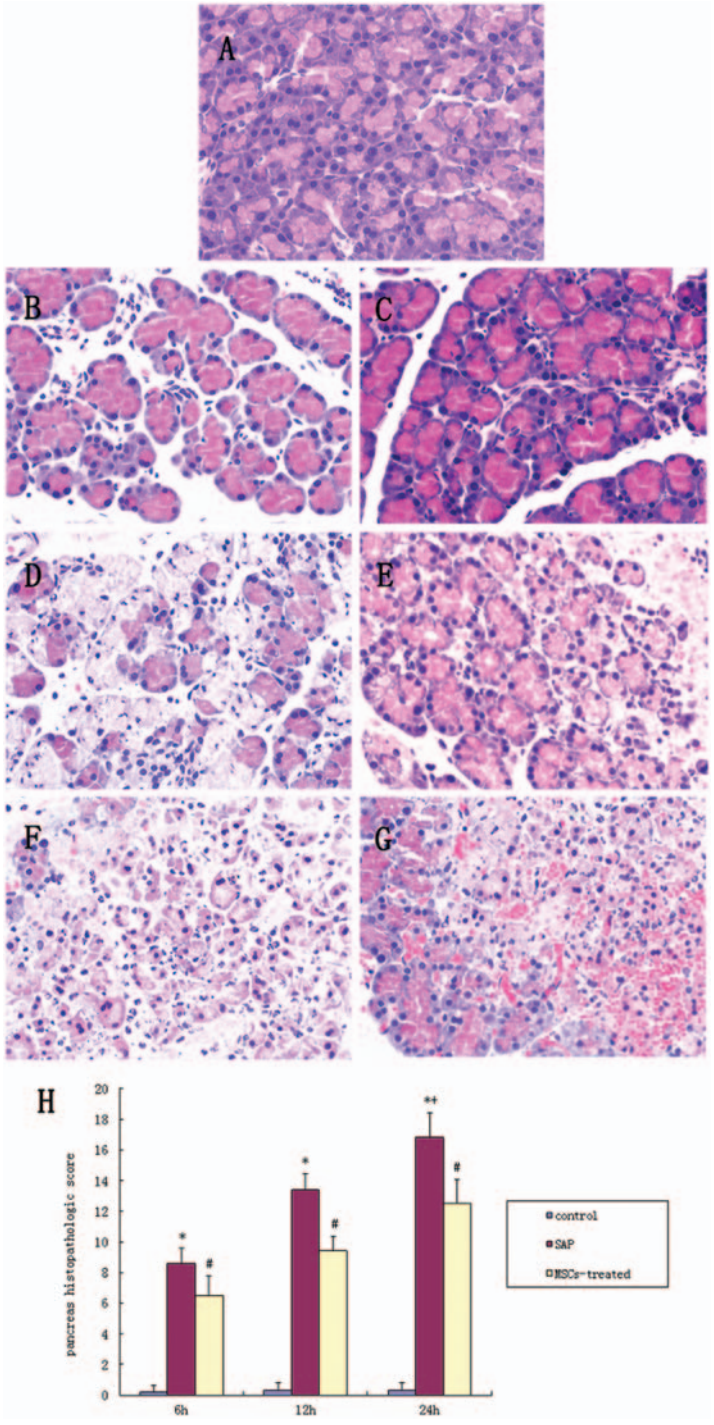

Figure 2 Histopathology of pancreas. In the control groups, the pancreatic parenchyma assumed typical normal architecture without interstitial oedema (A). The pancreatic lobular structures were overall normal with mild interstitial oedema and a few inflammatory cells infiltrated in the SAP groups at 6 h (B). In the SAP groups at 12 h, the change of pancreatic histopathology included interstitial oedema with acute inflammatory cell infiltration, glands damage, vacuolation and some acinar cells necrosis (D). Compared to the SAP groups at 12 h, the pancreatic damage more severe in the SAP groups at 24 h (F). After receiving MSCs treatment, the pancreatic damage was less severe than that in the SAP groups at the corresponding time point (C, E, and G). Pancreatic histological score are shown as the means ± SE ($n = 10$ rats per group). $^{+}P < 0.01$ compared in all SAP groups, $^{*}P < 0.01$ vs. the control groups at the same time point and $\#P < 0.01$ vs. the SAP groups at the same time point, as tested by two sample *t*-test for comparison between two groups, and one-way ANOVA for comparison among several groups (Figure 3H). Original magnification ×200

Ultrastructual examination of kidney

The change of renal capillary endothelial barrier was observed by using the TEM. The damage of renal capillary endothelial barrier was aggravated over time after induction of SAP. And the damage at 24 h was the most severe at all time points. After treatment with MSCs, the damage was lighter than that in the SAP groups at corresponding time points, respectively (Figure 3).

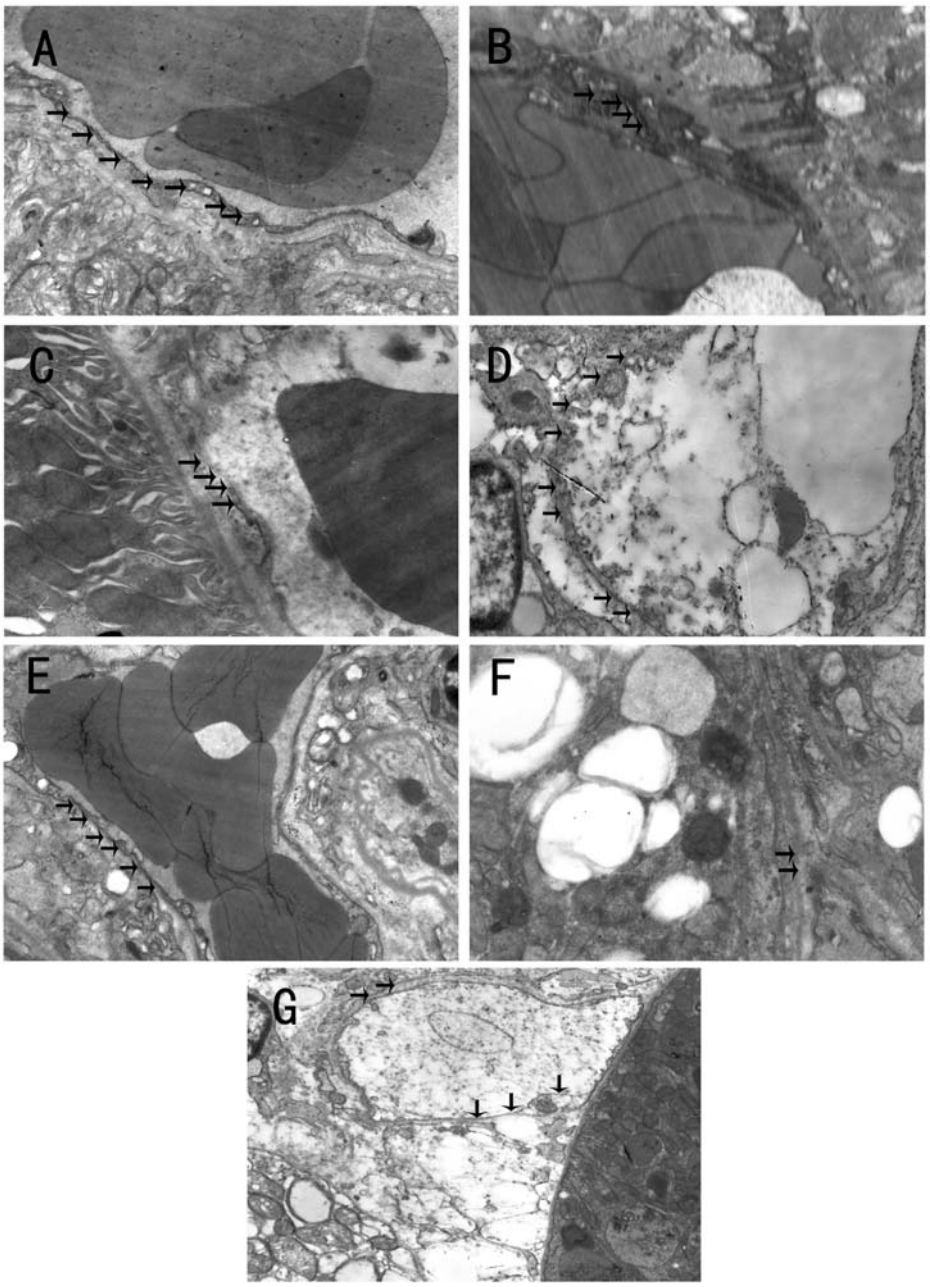

Figure 3 Ultrastructural examination of kidney. In the control groups, the capillary endothelial cells in the renal interstitium were complete and not impaired (A). In the SAP groups at 6 h, swelling of endothelial cells was noted in the capillaries without shedding (B). In the SAP groups at 12 h, focal shedding of capillary endothelial cells was noted (C). In the SAP groups at 24 h, extensive swelling, necrosis and shedding of capillary endothelial cells were observed under an electron microscope (D). After treatment with MSCs, the capillary endothelial cells showed no obvious impairment at 6 h (E). The numbers of capillary endothelial cells fell a little, but the damage was lighter than that in the SAP groups at 12 h (F). Capillary endothelial cells which were necrotic and shed were scattered in many places, but the level of damage was still lighter than that at 24 h (G). Original magnification $\times 8000$

Renal AQP1 expression

The immunohistochemical results showed that AQP1 expressed predominantly on the plasmalemma of epithelial cells in renal tubule (Figure 4A). Compared with the control groups, the expression of AQP1 decreased significantly at 24 h after induction of SAP (Figure 4B). After treatment with MSCs, the expression of AQP1 was higher than that in the SAP groups at the corresponding time points (Figure 4C).

By using the Western blot analysis, after induction of SAP, the level of renal AQP1 decreased significantly over time ($F = 74.85$, $P < 0.01$). After treatment with MSCs, the level of renal AQP1 was higher than that in the SAP groups at the corresponding time points, respectively (6 h: $t = 3.48$, $P < 0.05$; 12 h: $t = 3.0$, $P < 0.05$; 24 h: $t = 3.01$, $P < 0.05$) (Figure 4E).

Renal AQP1 mRNA expression

After induction of SAP, the transcript level of renal AQP1 mRNA decreased significantly over time ($F = 26.58$,

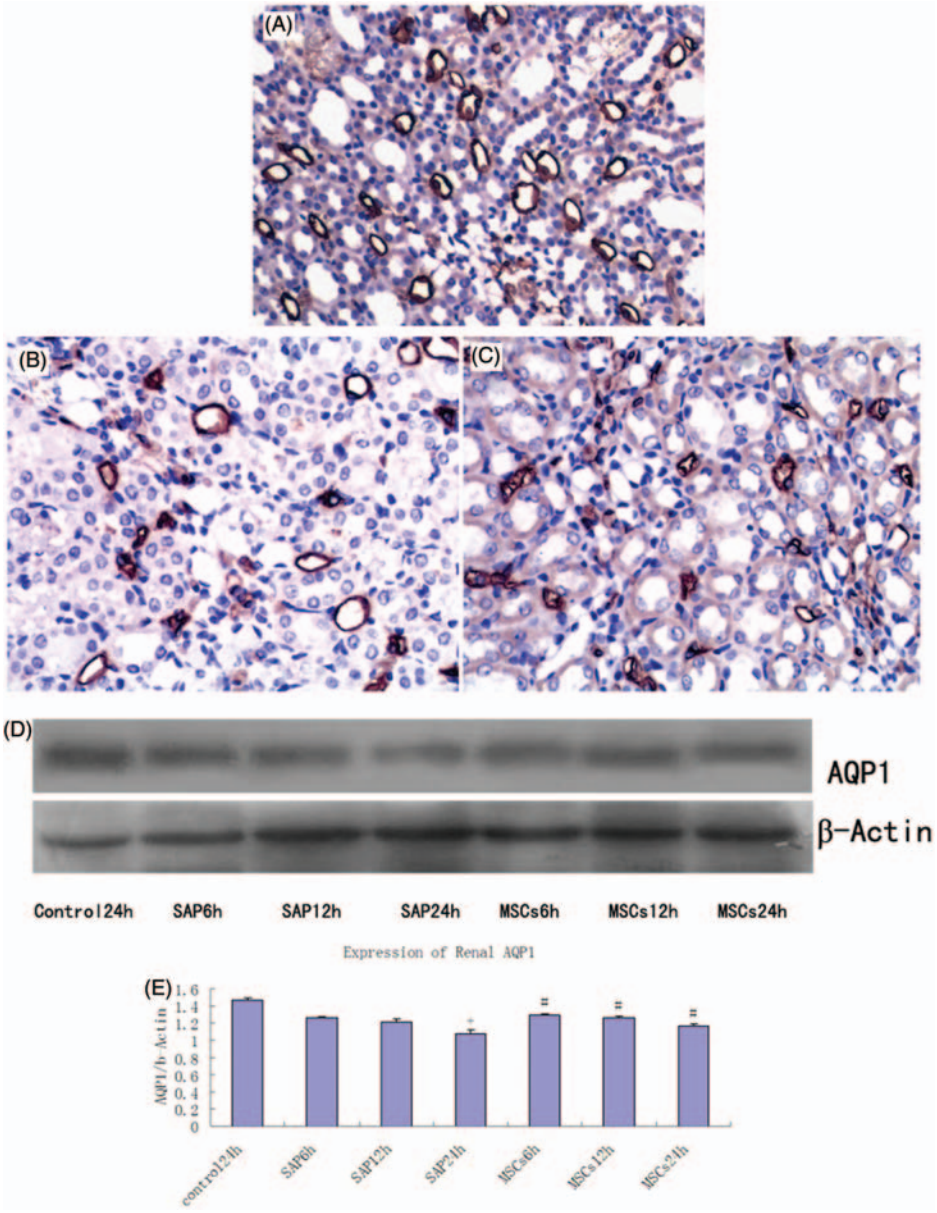

Figure 4 Renal AQP1 expression. In the control groups, the expression of AQP1 was noted predominantly on the plasmalemma of the epithelial cells in the renal tubules (A). Compared with the control groups, the expression of AQP1 decreased significantly in the SAP groups at 24 h (B). However, the expression of AQP1 in the MSCs-treated groups was higher than that in the SAP groups at 24 h (Figure 4C). Original magnification ×200. The Western blot analysis was used to determine the changes in the expression of renal AQP1 (D and E). $+P < 0.01$ compared in the control groups at 24 h and all SAP groups, and $\#P < 0.05$ vs. the SAP groups at the same time points, as tested using a two-sample *t*-test for comparing between two groups, and one-way ANOVA for comparing in several groups

$P < 0.01$). At 12 h and 24 h, the level of renal AQP1 mRNA was lower than that in the control groups, respectively (12 h: $t = 4.13$, $P < 0.05$; 24 h: $t = 5.84$, $P < 0.05$). After treatment with MSCs, the level of AQP1 mRNA was higher than that in the SAP groups at 12 h and 24 h, respectively (12 h: $t = 2.80$, $P < 0.05$; 24 h: $t = 3.34$, $P < 0.05$) (Table 2).

Table 2 Renal AQP1 mRNA expression

$2^{-\Delta\Delta CT}$	6 h	12 h	24 h
Control	1.02 ± 0.12	0.97 ± 0.12	0.95 ± 0.13
SAP	$0.70 \pm 0.06^{*}$	$0.60 \pm 0.04^{*}$	$0.38 \pm 0.03^{*\dagger}$
MSCs-treated	$0.80 \pm 0.07^{\ddagger}$	$0.68 \pm 0.02^{\ddagger}$	$0.50 \pm 0.04^{\ddagger}$

After induction of SAP and treatment with MSCs, quantitative RT-PCR was used to estimate changes in the expression of renal mRNA.
$^{*}P < 0.05$ vs. the control groups at the same time points.
$^{\dagger}P < 0.01$ compared in all SAP groups.
$^{\ddagger}P < 0.05$ vs. the SAP groups at the same time points, as tested using a two-sample *t*-test for comparing between two groups, and one-way ANOVA for comparing in several groups.

Discussion

In early stage, the over-release of inflammatory cytokines and the damage of capillary endothelial barrier appeared to be critical events in the etiopathology of SAP.[2–4] The endothelial cells of capillaries and the intercellular conjunctions

among endothelial cells are the functional basis of endothelial barrier, and the damage to these cells and their conjunctions may directly cause impairment of the endothelial barrier, leading to exudation of macromolecules in the capillaries, leakage of water into interstitial space, systemic oedema and reduction of effective circulating blood volume and insufficient perfusion of important organs including brain and heart, which subsequently lead to dysfunctions of these organs. Studies have demonstrated that improving the microcirculation in the lung and kidney may effectively improve the pathology and reduce the mortality in SAP.[13] The aforementioned studies have indirectly indicated that keeping the effective circulating blood volume was important in treatment of multiple organs injury in SAP. Moreover, the integrity of endothelial barrier played a critical role in keeping circulating blood volume. In our research, it was found that the damage of renal capillary endothelial barrier was positively correlated to the severity of the renal dysfunction.

AQP1, which could selectively mediate the water transportation,[5] was first reported by Agre *et al*.[14] It has a ubiquitous existence in various tissues, especially in kidney tissue. In kidney, it existed in the proximal convoluted tubule, proximal straight tubule and thin descending limb of Henle's loop and played an important role in renal reabsorption.[15] Studies have shown that abnormal expression of AQP1 was closely related to multiple renal diseases.[16–19]

According to the immunohistochemical analysis, we found the AQP1 mainly expressed in the endothelial membrane of renal tube. The results of quantitative PCR and Western blot analysis revealed that the expression of AQP1 in kidney was reversely time-dependent. The results suggested that the decrease of AQP1 might lead to the decrease of renal reabsorption, which could result in the reduction of circulating blood volume and then the renal blood circulation, eventually leading to worsened severity of the renal injury.

The MSCs, which belong to a class of mesodermal pluripotent stem cells, were abundant in the bone marrow and could be expanded extensively *in vitro*. The studies have confirmed that it could differentiate into a range of cell types such as adipocytes, osteoblasts, nerve cells, liver cells under different conditions.[20–22] In our research, the results of the FACS showed that the cells expressed high levels of CD29/CD90, and low levels of CD34/CD45. The results were comparable to what described by other researches[23] and confirmed that the cells cultured were the MSCs.

The animal experiments and clinical studies have shown that the MSCs could reduce the expression of various inflammatory factors,[24,25] inhibit immune responses[26,27] and promote the repairing of various tissues and organ injury.[28–30] In our research, after MSCs injection, the serum AMY, Cr and BUN levels decreased significantly. By transmission electron microscopy, we found that the damage of renal interstitial capillary was ameliorated. Furthermore, the decrease of AQP1 was significantly inhibited after treatment with MSCs.

According to this comprehensive study, we hypothesize that MSCs could reduce fluid loss by ameliorating the damage of renal interstitial capillary and increase fluid reabsorption by reversing the decrease of AQP1 in kidney. These could alleviate renal microcirculation disorder induced by SAP.

Author contributions: HH designed and guided the research; ZC performed the research, analysed data and wrote the manuscript; FL performed the research and supplied critical reagents; HF performed the research and collected data.

ACKNOWLEDGEMENTS

The study was supported by grants from National Natural Science Foundation of China (No.81070369). We thank Dr. Xingfeng Qi and Dr. Xisheng Xiong (Department of Pathology, Fuzhou General Hospital of Nanjing Military Command) for pathological examination and Dr. Xi Lin (Center of Transmission Electron Microscope Technology, Fujian Medical University) for TEM technical support.

REFERENCES

1. Pupelis G. Renal failure in acute pancreatitis. Timing of dialysis and surgery. *Przegl Lek* 2000;**57**:29–31
2. Cappell MS. Acute pancreatitis: etiology, clinical presentation, diagnosis, and therapy. *Med Clin North Am* 2008;**92**:889–923
3. Al Mofleh IA. Severe acute pancreatitis: pathogenetic aspects and prognostic factors. *World J Gastroenterol* 2008;**14**:675–84
4. Eibl G, Hotz HG, Faulhaber J, Kirchengast M, Buhr HJ, Foitzik T. Effect of endothelin and endothelin receptor blockade on capillary permeability in experimental pancreatitis. *Gut* 2000;**46**:390–4
5. Verkman AS. Physiological importance of aquaporin water channels. *Ann Med* 2002;**34**:192–200
6. Kes P, Vucicević Z, Ratković-Gusić I, Fotivec A. Acute renal failure complicating severe acute pancreatitis. *Ren Fail* 1996;**18**:621–8
7. Nishiwaki H, Ko I, Hima A, Ha SS, Satake K, Sowa M. Renal microcirculation in experimental acute pancreatitis of dogs. *Ren Fail* 1993;**15**:27–31
8. Feng DX, Peng W, Chen YF, Chen T, Tian JY, Si HR, Cai J, Rao Y, Han F, Zhao R. Down-regulation of aquaporin 1 in rats with experimental acute necrotizing pancreatitis. *Pancreas* 2012;**41**:1092–8
9. Gerson SL. Mesenchymal stem cells: no longer second class marrow citizens. *Nat Med* 1999;**5**:262–4
10. Cui HF, Bai ZL. Protective effects of transplanted and mobilized bone marrow stem cells on mice with severe acute pancreatitis. *World J Gastroenterol* 2003;**9**:2274–7
11. Schmidt J, Rattner DW, Lewandrowski K. A better model of acute pancreatitis for evaluating therapy. *Ann Surg* 1992;**215**:44–56
12. The Ministry of Science and Technology of the People's Republic of China. *Guidance Suggestion of Caring Laboratory Animals*. Beijing: Author, 2006
13. Foitzik T, Eibl G, Hotz HG, Faulhaber J, Kirchengast M, Buhr HJ. Endothelin receptor blockade in severe acute pancreatitis leads to systemic enhancement of microcirculation, stabilization of capillary permeability, and improved survival rates. *Surgery* 2000;**128**:399–407
14. Agre P, Preston GM, Smith BL, Jung JS, Raina S, Moon C, Guggino WB, Nielsen S. Aquaporin CHIP: the archetypal molecular water channel. *Am J Physiol* 1993;**265**:F463–76
15. Hara-Chikuma M, Verkman AS. Aquaporin-1 facilitates epithelial cell migration in kidney proximal tubule. *J Am Soc Nephrol* 2006;**17**:39–45
16. Bachinsky DR, Sabolic I, Emmanouel DS, Jefferson DM, Carone FA, Brown D, Perrone RD. Water channel expression in human ADPKD kidneys. *Am J Physiol* 1995;**268**:F398

17. Kim SW, Cho SH, Oh BS, Yeum CH, Choi KC, Ahn KY, Lee J. Diminished renal expression of aquaporin water channels in rats with experimental bilateral ureteral obstruction. *J Am Soc Nephrol* 2001;**12**:2019–28
18. Kwon TH, Frøkiaer J, Fernández-LIama P, Knepper MA, Nielsen S. Reduced abundance of aquaporins in rats with bilateral ischemia-induced acute renal failure: prevention by alpha-MSH. *Am J Physiol* 1999;**277**:F413–27
19. Kim SW, Lee JU, Nah MY, Kang DG, Ahn KY, Lee HS, Choi KC. Cisplatin decreases the abundance of aquaporin water channels in rat kidney. *J Am Soc Nephrol* 2001;**12**:875–82
20. Vieyra DS, Jackson KA, Goodell MA. Plasticity and tissue regenerative potential of bone marrow-derived cells. *Stem Cell Rev* 2005;**1**:65–9
21. Meirelles LS, Nardi NB. Murine marrow-derived mesenchymal stem cell: isolation, *in vitro* expansion, and characterization. *Br J Haematol* 2003;**123**:702–11
22. Lagasse E, Connors H, Al-Dhalimy M, Reitsma M, Dohse M, Osborne L, Wang X, Finegold M, Weissman IL, Grompe M. Purified hematopoietic stem cells can differentiate into hepatocytes *in vivo*. *Nat Med* 2000;**6**:1229–34
23. Kemp EC, Hows J, Donaldson C. Bone marrow-derived mesenchymal stem cells. *Leuk Lymphoma* 2005;**46**:1531–44
24. Hagiwara M, Shen B, Chao L, Chao J. Kallikrein-modified mesenchymal stem cell implantation provides enhanced protection against acute ischemic kidney injury by inhibiting apoptosis and inflammation. *Hum Gene Ther* 2008;**19**:807–19
25. Jung KH, Song SU, Yi T, Jeon MS, Hong SW, Zheng HM, Lee HS, Choi MJ, Lee DH, Hong SS. Human bone marrow-derived clonal mesenchymal stem cells inhibit inflammation and reduce acute pancreatitis in rats. *Gastroenterology* 2011;**140**:998–1008
26. Garcia-Olmo D, Garcia-Arranz M, Herreros D, Pascual I, Peiro C, Rodríguez-Montes JA. A phase I clinical trial of the treatment of Crohn's fistula by adipose mesenchymal stem cell transplantation. *Dis Colon Rectum* 2005;**48**:1416–23
27. English K, Barry FP, Mahon BP. Murine mesenchymal stem cells suppress dendritic cell migration, maturation and antigen presentation. *Immunol Lett* 2008;**115**:50–8
28. Sémont A, Franois S, Mouiseddine M. Mesenchymal stem cells increase self-renewal of small intestinal epithelium and accelerate structural recovery after radiation injury. *Adv Exp Med Biol* 2006;**585**:19–30
29. Orlic D, Kajstura J, Chinenti S, Jakoniuk I, Anderson SM, Li B, Pickel J, McKay R, Nadal-Ginard B, Bodine DM, Leri A, Anversa P. Bone marrow cells regenerate infracted myocardium. *Nature* 2001;**410**:701–5
30. Deng YB, Yuan QT, Liu XG, Liu XL, Liu Y, Liu ZG, Zhang C. Functional recovery after rhesus monkey spinal cord injury by transplantation of bone marrow mesenchymal-stem cell-derived neurons. *Chin Med J (Engl)* 2005;**118**:1533–41

(Received October 21, 2012, Accepted January 28, 2013)